Journal of Pharmaceutical Sciences 112 (2023) 3216–3223

Contents lists available at ScienceDirect

Journal of Pharmaceutical Sciences

journal homepage: www.jpharmsci.org

Pharmacokinetics, Pharmacodynamics and Drug Transport and Metabolism

Development and Functional Evaluation of MDR1-expressing Microvascular Endothelial-like Cells Derived from Human iPS Cells as an *In vitro* Blood-brain Barrier Model

Tomoko Yamaguchi[a,1], Daiki Sako[b,1], Toshiki Kurosawa[b], Misae Nishijima[a], Ayaka Miyano[c], Yoshiyuki Kubo[b], Sumio Ohtsuki[c,d], Kenji Kawabata[a,e,f,**], Yoshiharu Deguchi[b,*]

[a] *Laboratory of Cell Model for Drug Discovery, National Institutes of Biomedical Innovation, Health and Nutrition, 7-6-8 Saito-Asagi, Ibaraki, 567-0085, Japan*
[b] *Laboratory of Drug Disposition & Pharmacokinetics, Faculty of Pharma-Sciences, Teikyo University, 2-11-1 Kaga, Itabashi, Tokyo 173-8605, Japan*
[c] *Department of Pharmaceutical Microbiology, Graduate School of Pharmaceutical Sciences, Kumamoto University, 5-1 Oe-Honmachi, Chuo-Ku, Kumamoto 862-0973, Japan*
[d] *Department of Pharmaceutical Microbiology, Faculty of Life Sciences, Kumamoto University, 5-1 Oe-Honmachi, Chuo-Ku, Kumamoto 862-0973, Japan*
[e] *Laboratory of Biomedical Innovation, Graduate School of Pharmaceutical Sciences, Osaka University, 1-6 Yamadaoka, Suita 565-0871, Japan*
[f] *Department of Microbiology and Immunology, Kobe University Graduate School of Medicine, 7-5-1, Kusunoki-cho, Chuo-ku, Kobe 650-0017, Japan*

ARTICLE INFO

Article history:
Received 11 July 2023
Revised 4 September 2023
Accepted 5 September 2023
Available online 9 September 2023

Keywords:
Blood-brain barrier
ABC transporter
SLC transporter
Human induced pluripotent stem cells
P-glycoprotein

ABSTRACT

In order to establish an *in vitro* model of the human blood-brain barrier (BBB), MDR1-overexpressing human induced pluripotent stem cells (hiPSCs) were generated, and they were differentiated to MDR1-expressing brain microvascular endothelial-like cells (MDR1-expressing hiPS-BMECs). MDR1-expressing hiPS-BMECs monolayers showed good barrier function in terms of tight junction protein expression and trans-epithelial electrical resistance (TEER). In sequential window acquisition of all theoretical fragment ion spectra mass spectrometry (SWATH-MS), MDR1 protein expression was markedly increased in MDR1-expressing hiPS-BMECs, whereas other ABC and SLC transporters showed almost identical expression between MDR1-expressing hiPS-BMECs and mock hiPS-BMECs, suggesting that MDR1 overexpression had little or no knock-on effect on other proteins. The basolateral-to-apical transport of MDR1 substrates, such as quinidine, [^{3}H]digoxin and [^{3}H]vinblastine, was higher than the apical-to-basolateral transport, and the efflux-dominant transport was attenuated by PSC833, an MDR1-specific inhibitor, indicating that MDR1-mediated efflux transport is functional. The robust MDR1 function was also supported by the efflux-dominant transports of [^{3}H]cyclosporin A, loperamide, cetirizine, and verapamil by MDR1-expressing hiPS-BMECs. These results suggest that MDR1-expressing hiPS-BMECs can be used as an *in vitro* model of the human BBB.

Introduction

The blood-brain barrier (BBB), which regulates the transport of molecules between the central nervous system (CNS) and peripheral circulation, is mainly composed of brain microvascular endothelial cells (BMECs), pericytes, and astrocytes. The formation of tight junctions and expression of efflux/influx transporters are characteristic features of BMECs.[1] BBB models are required for studies of drug transport at the BBB and for the development of drugs that can reach the CNS. In early studies, *in vitro* BBB models were developed using

* Corresponding author at: Laboratory of Drug Disposition & Pharmacokinetics, Faculty of Pharma-Sciences, Teikyo University, 2-11-1 Kaga, Itabashi, Tokyo 173-8605, Japan.
** Corresponding author at: Laboratory of Cell Model for Drug Discovery, National Institutes of Biomedical Innovation, Health and Nutrition, 7-6-8 Saito-Asagi, Ibaraki, 567-0085, Japan.
E-mail addresses: kawabata@nibiohn.go.jp (K. Kawabata), deguchi@pharm.teikyo-u.ac.jp (Y. Deguchi).
[1] Tomoko Yamaguchi and Daiki Sako contributed equally to this work.

https://doi.org/10.1016/j.xphs.2023.09.004

cultured animal-derived BMECs,[2-4] but the expression pattern and levels of transporters differ from those of human BMECs.[5-8] Therefore, human primary BMECs and immortalized human cell lines have been employed for the study of drug transport across the human BBB in spite of a number of disadvantages, such as limited supply, inter-lot variation, and weak tight junctions. In particular, hCMEC/D3 cells, an *in vitro* model cell line of human BMECs, retain many of the morphological and functional characteristics of the human BBB in terms of expression of multiple transporters.[9,10] However, hCMEC/D3 cells have low TEER values (30-50 $\Omega \times cm^2$), making it difficult to study the transcellular transport of low-molecular-weight compounds.[9,11] In this context, the generation of brain microvascular endothelial-like cells from human induced pluripotent stem cells (hiPS-BMECs) was reported by Lippmann *et al.*[12,13] Recently, our group also reported hiPS-BMECs with BBB-like characteristics, including the formation of strong tight junctions and the expression of various drug and nutrient transporters.[14-17]

Among these transporters, multidrug resistance protein1 (MDR1, P-glycoprotein), encoded by human *ABCB1* gene, is highly expressed in various organs, such as the small intestine and the BBB. Since MDR1 plays an important role in the efflux of various drugs, it is essential to evaluate whether CNS drug candidates are potential MDR1 substrates.[18] Unfortunately, MDR1 expression in hiPS-BMECs is significantly lower than that in hCMEC/D3 cells.[14,19] In addition, our previous report on the transcellular transport of quinidine, an MDR1 substrate, showed no significant difference between transport in the apical-to-basolateral (A-to-B) and basolateral-to-apical (B-to-A) directions in hiPS-BMECs.[14] Therefore, the successful upregulation of MDR1 expression in hiPS-BMECs could provide a new human BBB model with tight junctions and appropriate efflux transport function, that is, both physical and functional barriers. Such a model would be useful in drug development and fundamental studies of the BBB. Although we recently reported upregulation of MDR1 expression by Wnt signaling and SRY-box transcription factor 18 (Sox18) overexpression in hiPS-BMECs, MDR1 expression remained lower than that in primary human BMECs or hCMEC/D3 cells.[20,21]

Thus, the aim of the present study was to develop MDR1-overexpressing hiPSCs and differentiate them to MDR1-expressing hiPS-BMECs, and to examine the expression and function of MDR1 in the obtained cells. In addition, several representative ATP-binding cassette (ABC) and solute carrier (SLC) transporters expressed in hiPS-BMECs were examined, in line with our previous work.[14,17]

Methods

Reagents

Compounds of reagent grade were purchased from FUJIFILM Wako Pure Chemical Industries (Osaka Japan), Sigma-Aldrich Company (St. Louis, MO), Tokyo Chemical Industry (Tokyo, Japan). L-[2,3,4-^{3}H]Arginine ([^{3}H]L-arginine, 40 Ci/mmol), [MEBMT-β-^{3}H] cyclosporin A ([^{3}H]cyclosporin A, 20 Ci/mmol), and [^{3}H(G)]vinblastine sulfate ([^{3}H]vinblastine, 20 Ci/mmol) were purchased from American Radiolabeled Chemicals (St. Louis, MO). L-[^{14}C(U)]Lactic acid sodium salt ([^{14}C]L-lactate, 150.6 mCi/mmol), [^{3}H(G)]digoxin ([^{3}H]digoxin, 23.8 Ci/mmol) and L-[3,4,5-^{3}H(N)]leucine ([^{3}H]L-leucine, 72.56 Ci/mmol) were purchased from PerkinElmer (Waltham, MA). Details of the buffers are provided in the supplementary information.

Cell Culture

Human iPS cells (hiPSCs: iMR90-4)[22] were purchased from WiCell Research Institute (Madison, WI), and cultured in mTeSR1 medium (StemCell Technologies, Vancouver, Canada) on Matrigel^{TM}-coated 6-well plates (Thermo Fisher Scientific, Waltham, MA). hCMEC/D3 cells were cultured in EBM-2 medium (Lonza, Basel, Switzerland) supplemented with fetal bovine serum, growth factors (VEGF, R3-IGF, hEGF, hydrocortisone, FGF2), penicillin-streptomycin, and HEPES on collagen I-coated dishes, and were maintained at 37°C in an atmosphere of 95% air and 5% CO_2.

MDR1-Overexpressing hiPSCs

The CSII-EF-MCS-IRES-Venus lentiviral vector and packaging constructs (pCMV-VSV-G-RSV-Rev and pCAG-HIVgp) were purchased from the RIKEN BioResource Center. Human MDR1 complementary deoxyribonucleic acid (cDNA) was subcloned into the NotI/BamHI sites of CSII-EF-MCS-IRES-Venus (Fig. 1). Cells were infected with the vector according to the reported procedure.[23,24]

To produce MDR1-overexpressing hiPSCs, the cells were infected with lentiviruses, and the cells were dissociated using Accutase (Merck Millipore, Billerica, MA) and resuspended in mTeSR1 medium supplemented with 10 μM Y27632 (FUJIFILM Wako). Venus-positive cells were collected using SH800 (SONY) and seeded onto growth factor-reduced BD Matrigel Basement Membrane Matrix in mTeSR1 medium with Y27632. Twenty-four individual colonies were selected and reseeded onto Matrigel Basement Membrane Matrix 5 days post-sorting. Venus-positive cells were identified using flow cytometry after the cells had reached near-confluence. Three clones (1,3, and 9) were obtained, and clone #3 was selected here because it showed the highest transduction efficiency (Supplemental Fig. 1 for mRNA levels of MDR1 in each clone). To produce mock hiPSCs was infected with CSII-EF-MCS-IRES-Venus lentiviruses. Venus-positive cells were collected using SH800 and we obtained twenty-four individual colonies. Two clones (1 and 4) were selected and the results for clone #1 are described here. The culture method for MDR1-overexpressing hiPSCs and mock hiPSCs was the same as for non-transduced cells when the cells were used to prepare MDR1-expressing hiPS-BMECs and mock hiPS-BMECs (Fig. 1).

Differentiation to MDR1-Expressing hiPS-BMECs

Differentiation of MDR1-overexpressing hiPSCs and mock hiPSCs to MDR1-expressing hiPS-BMECs and mock hiPS-BMECs was conducted according to the reported method for the differentiation of hiPSCs to hiPS-BMECs.[12,13] On Day −3, MDR1-overexpressing hiPSCs were dissociated into single cells using Accutase. The single cells ($1.0\text{-}1.5 \times 10^5$ cells/well) were seeded on Matrigel^{TM}-coated 6-well plates and cultured in mTeSR1 with 10 μM Y27632. The medium

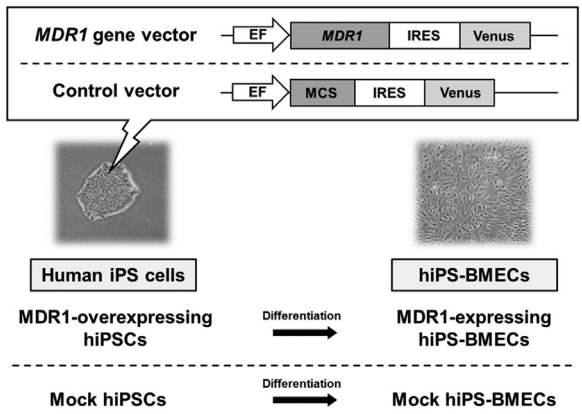

Figure 1. Establishment of MDR1-expressing hiPS-BMECs.
Lentiviral vectors with or without the *MDR1* gene were constructed to be introduced into hiPSCs. Each cell was differentiated by reported methods[12,13] to obtain MDR1-expressing hiPS-BMECs and mock hiPS-BMECs.

was replaced with fresh mTeSR1 medium without Y27632 after 24 h (Day −2). On Day 0, the medium was switched to unconditioned medium (supplementary information), then on Day 6, the medium was changed to human endothelial serum-free medium (ESFM; Thermo Fisher Scientific) containing 10 μM all-*trans*-retinoic acid (RA; FUJIFILM Wako), 20 ng/mL human fibroblast growth factor 2 (FGF2; Sigma-Aldrich Company) and 1% human serum from platelet-poor human plasma (hPDS; Sigma-Aldrich Company). On Day 8, the cells were dissociated with Accutase and seeded at 3.3×10^5 cells/cm^2 on 24-well Transwell™ polyester membranes with 0.4 μm pores (Corning, NY) coated with fibronectin/collagen IV (PharmaCo-Cell, Nagasaki, Japan). On Day 9, the medium was changed to ESFM + 1% hPDS without RA or bFGF2. The cells were used for experiments on Day 10. The TEER values of MDR1-expressing hiPS-BMECs was measured on Transwell™ inserts by use of Millicell ERS-2 (Merck Millipore), and the TEER values were calculated as described in previous studies.[20,25]

Quantitative Reverse Transcription-Polymerase Chain Reaction (qRT-PCR)

qRT-PCR using an Applied Biosystems 7500 Real-Time PCR System (Thermo Fisher Scientific) was performed as described previously.[14] Details of primers and cycle conditions are provided in the supplementary information. Total RNA was isolated using Nucleospin™ RNA plus (Macherey-Nagel, Germany), and complementary DNA (cDNA) was prepared by using SuperScript III Reverse Transcriptase (Thermo Fisher Scientific) and random primers according to the manufacturer's protocol. SYBR select master mix (Thermo Fisher Scientific) was used in PCR. The parameters were 1 cycle for uracil-DNA glycosylase (UDG) activation at 50°C for 2 min, 1 cycle for enzyme activation at 95°C for 10 min and 40 cycles of 95°C for 3 s, 60°C for 1 min for polymerase chain reaction. The expression of mRNA of interest was normalized according to the mRNA expression of TATA-box binding protein (TBP).

Quantitative Proteomics Analysis

Whole cell lysates prepared from hCMEC/D3 cells, mock hiPS-BMECs and MDR1-expressing hiPS-BMECs were extracted into extraction buffer containing 12 mM sodium deoxycholate and 12 mM sodium lauroyl sarcosinate (FUJIFILM Wako) in 100 mM Tris-HCl (pH 9.0). The protein amount was determined with a Micro BCA protein assay kit (Thermo Fisher Scientific). The cell lysates were digested by the phase-transfer surfactant method as previously described.[26,27] Briefly, reduction was carried out with 10 mM dithiothreitol at room temperature, then 550 mM iodoacetamide was added at room temperature in the dark. The samples were diluted 5-fold with 50 mM ammonium bicarbonate and digested with lysyl endopeptidase (FUJIFILM Wako) for 3 h. Subsequently, the samples were digested with trypsin (Promega, Madison, WI, USA) for 16 h. The detergents were removed by using ethyl acetate under acidic conditions, and the samples were desalted using GL-Tip SDB and GC (GL Sciences, Tokyo, Japan) and dried. The residue was reconstituted with 0.1% trifluoroacetic acid, and subjected to liquid chromatography-tandem mass spectrometry (LC-MS/MS). Samples were also analyzed by sequential window acquisition of all theoretical fragment ion spectra mass spectrometry (SWATH-MS) on a TripleTOF6600 (SCIEX, Framingham, MA, USA) interfaced with an Eksigent nanoLC400 (SCIEX). Protein identification and quantification were performed by DIA-NN 1.8 with the human reference proteome.[28]

Immunocytochemistry

Cells were fixed in 4% paraformaldehyde/PBS at room temperature for 15 min. Post-washing with PBS, the cell culture inserts were cut out using a scalpel (MANI ophthalmic knife; MANI). The cells were blocked with 10% normal goat serum (FUJIFILM Wako) in PBS supplemented with 0.1% Triton-X at room temperature for 1 h, incubated with mouse anti-MDR1 antibodies (final concentration, 4.0 μg/mL; Thermo Fisher Scientific) at 4°C overnight, then further incubated with Alexafluor594-conjugated secondary antibodies (final concentration, 2.0 μg/mL; Thermo Fisher Scientific) at room temperature for 1 h. Post-washing, the nuclei were labeled with 4', 6-diamidino-2-phenylindole (DAPI, Sigma-Aldrich Company) at room temperature for 10 min. Cell culture inserts were mounted using ProLong Diamond Antifade Mountant (Thermo Fisher Scientific). Images were captured using an LSM 700 microscope (Carl Zeiss, Germany) at 63× magnification, excitation 405 nm for DAPI, 555 nm for Alexafluor594.

Evaluation of Drug Permeability

Drug permeability or transport was examined as described previously.[14,16] On Day 10, the culture medium was replaced with assay buffer, 200 μL for the upper chamber and 900 μL for the bottom chamber to perform preincubation for 30 min at 37°C, and assay were initiated by adding buffer containing a test compound to the upper or bottom chamber. In the case of inhibition analysis, inhibitor was added to the upper and bottom chambers at the start of preincubation. Quantification of test drugs using LC-MS/MS and measurement of the radio-labeled compounds were carried out as described previously,[14,17] and in the supplementary information. Sodium fluorescein (NaF) in the sample was determined using a fluorescence multiwell plate reader (Genios, TECAN). The apparent permeability coefficient (P_{app}) was calculated as described in the supplementary information.

Statistical Analysis

Statistical analysis was performed using Student's *t*-test and one-way ANOVA with Dunnett's or Tukey's test.

Results

Generation of MDR1-Overexpressing hiPSCs

Comparison of bright-field images indicated that the cellular morphology of MDR1-overexpressing hiPSCs was not different from that of untransduced hiPSCs or mock hiPSCs (Fig. 2A). The expression levels of Venus, an indicator of exogenous gene expression, in the mock hiPSCs and MDR1-overexpressing hiPSCs were significantly higher than that of untransduced cells (Fig. 2B). The expression of Venus in MDR1-overexpressing hiPSCs was lower than that in mock hiPSCs, presumably because of its co-expression with MDR1. In addition, the mRNA expression level of MDR1 was significantly increased in MDR1-overexpressing hiPSCs (Fig. 2C), while the mRNA expression levels of undifferentiated marker genes, such as Nanog and Oct3/4, remained unchanged across all groups, supporting the view that the mock hiPSCs and MDR1-overexpressing hiPSCs were undifferentiated (Fig. 2D).

Effect of MDR1 Overexpression on Barrier Function and Endothelial Cell Marker Expression

hiPS-BMECs are known to form tight junctions, which is a characteristic feature of BMECs, and we next examined the effect of MDR1

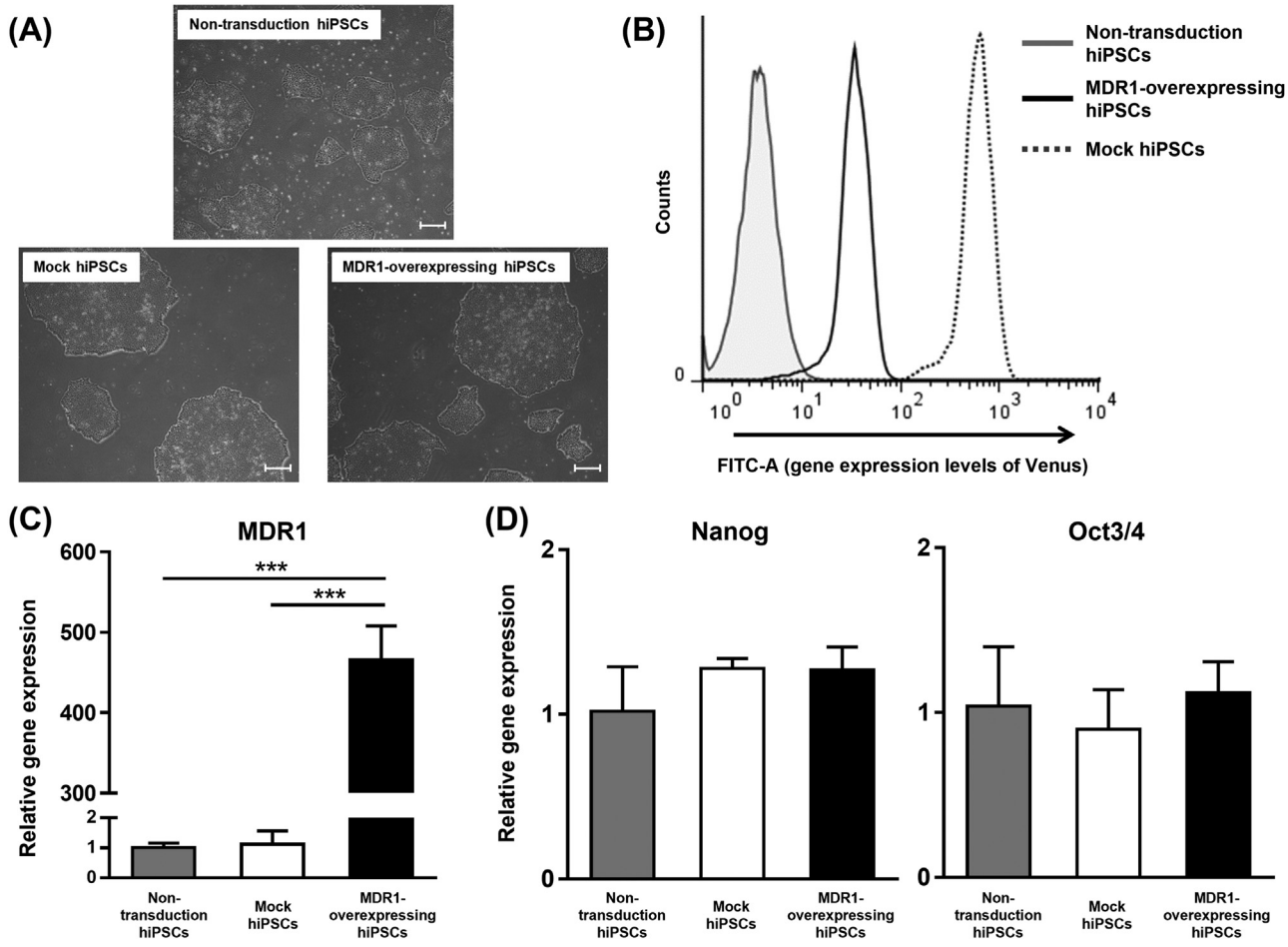

Figure 2. Expression of undifferentiated markers in MDR1-overexpressing hiPSCs. (A) Phase-contrast micrographs of undifferentiated hiPSCs. Scale bar: 300 μm. (B) Gene expression levels of Venus were measured using flow cytometry. (C) Gene expression levels of *MDR1* were measured using qRT-PCR. (D) Gene expression levels of Nanog and Oct3/4 in undifferentiated hiPSCs were measured using qRT-PCR. The gene expression levels in the non-transduction hiPSCs were set to 1.0. Statistical significance was calculated using the unpaired Student's *t*-test (***$p < 0.001$). Gray, white, and black columns represent non-transduction, mock and MDR1-overexpressing hiPSCs, respectively. Data are presented as the mean ± SD from three independent experiments (n = 3).

overexpression on BBB integrity and paracellular permeability by measuring TEER and NaF flux as paracellular markers. The mock hiPS-BMECs and MDR1-expressing hiPS-BMECs showed no significant difference in TEER values (Fig. 3A), and MDR1 overexpression also had no significant effect on NaF transcellular transport in these two cell lines (Fig. 3B). In addition, the mock hiPS-BMECs and MDR1-expressing hiPS-BMECs showed no significant differences in the expression levels of tight junction-related genes, such as claudin-5, occludin, and ZO-1 (Fig. 3C). These results suggest that MDR1 overexpression had no effect on the physical barrier function of hiPS-BMECs. Furthermore, there was no difference in cellular morphology between the mock hiPS-BMECs and MDR1-expressing hiPS-BMECs (Fig. 3D), and there was also no difference in the expression of genes encoding endothelial cell markers, such as PECAM1 and VE-cadherin (Fig. 3E).

Effect of MDR1 Overexpression on Various Transporters in MDR1-Expressing hiPS-BMECs

SWATH-MS analysis revealed that MDR1 protein expression was markedly increased in MDR1-expressing hiPS-BMECs, whereas other ABC and SLC transporters showed almost identical expression levels in MDR1-expressing hiPS-BMECs and mock hiPS-BMECs (Fig. 4A). This result suggests that overexpression of MDR1 has no significant effect on the expression of the other ABC and SLC transporters originally present in hiPS-BMECs. In addition, immunocytochemical examination showed that the signal of MDR1 protein was detected at the apical membrane of MDR1-expressing hiPS-BMECs, while there was no signal at this location in mock hiPS-BMECs (Fig. 4B).

Comparison of Protein Expression levels in MDR1-Expressing hiPS-BMECs and hCMEC/D3 Cells

To ascertain the usefulness of MDR1-expressing hiPS-BMECs as human BBB model cells, the protein expression levels were compared in MDR1-expressing hiPS-BMECs and hCMEC/D3 cells, typical human BBB cells, using the SWATH-MS method. SWATH-MS detected 6077 proteins in MDR1-expressing hiPS-BMECs and hCMEC/D3 cells (Fig. 5A). For 90.8% of the proteins detected, the expression levels were within a 10-fold difference range in the two cell lines. In particular, the MDR1 protein level in MDR1-expressing hiPS-BMECs was similar to that in hCMEC/D3 cells (Fig. 5B). Other transporter expression levels were within a 10-fold difference, except for glucose transporter 3 (GLUT3/SLC2A3).

Evaluation of MDR1 Function in MDR1-Expressing hiPS-BMECs Monolayer

In the permeability experiments, transport of MDR1 substrates such as quinidine, [^{3}H]digoxin, [^{3}H]vinblastine was the same in the

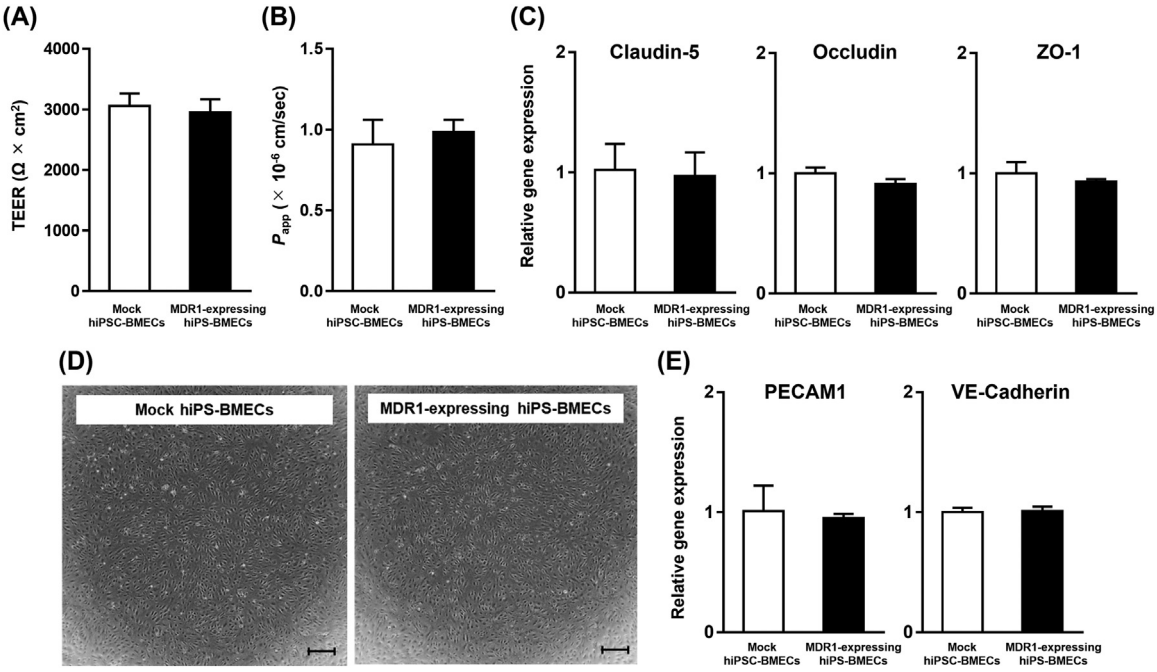

Figure 3. The barrier function of MDR1-expressing hiPS-BMECs. (A) TEER values in mock hiPS-BMECs and MDR1-expressing hiPS-BMECs. (B) NaF flux across the cell monolayer. (C) Measurement of the expression levels of claudin-5, occludin, and ZO-1 using qRT-PCR. The gene expression levels in the mock hiPS-BMECs were set to 1.0. (D) Phase-contrast micrographs of hiPS-BMECs. Scale bar: 300 μm. (E) Measurement of the gene expression levels of PECAM1 and VE-cadherin using qRT-PCR. The gene expression levels in the mock hiPS-BMECs were set to 1.0. White and black columns represent mock and MDR1-expressing hiPS-BMECs, respectively. Data are presented as the mean ± SD from three independent experiments (n = 3).

A-to-B and B-to-A directions in mock hiPS-BMECs, whereas MDR1-expressing hiPS-BMECs showed B-to-A dominant asymmetric transport. In the inhibition study, B-to-A dominant transport of quinidine, [^{3}H]digoxin and [^{3}H]vinblastine was significantly inhibited by 10 μM PSC833, a specific MDR1 inhibitor (Fig. 6A-C).

As shown in Fig. 6D, ER values of MDR1 substrates, such as [^{3}H]vinblastine, [^{3}H]digoxin, [^{3}H]cyclosporin A, quinidine, loperamide, cetirizine, erlotinib and verapamil, all showed significantly higher than those of mock hiPS-BMECs (26.0, 11.1, 9.25, 2.21, 2.14, 2.00, 1.86 and 1.52, respectively), and their efflux ratio (ER) values were significantly decreased by 10 μM PSC833. On the other hand, PSC833 had no prominent effect for risperidone.

Functional Evaluation of SLC Transporters in MDR1-Expressing hiPS-BMECs and Mock hiPS-BMECs Monolayer

The function of SLC transporters was next analyzed in mock hiPS-BMECs and MDR1-expressing hiPS-BMECs (Table 1). First, the permeability, P_{app} was evaluated in the A-to-B and B-to-A directions. Mock hiPS-BMECs and MDR1-expressing hiPS-BMECs showed similar values of P_{app} for [^{3}H]L-arginine, [^{14}C]L-lactate, [^{3}H]L-leucine and [^{3}H]L-glutamate (Table 1). The ERs were calculated from the obtained P_{app} values. Mock hiPS-BMECs and MDR1-expressing hiPS-BMECs showed comparable ER values for [^{3}H]L-arginine (0.754, 0.780, respectively), [^{14}C]L-lactate (0.0799, 0.0711), [^{3}H]L-leucine (0.907, 0.829) and [^{3}H]

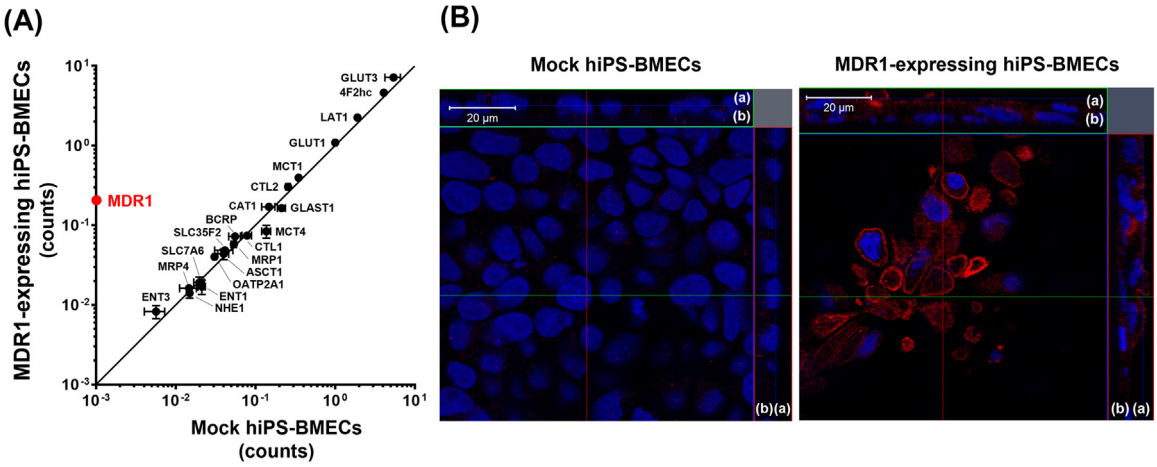

Figure 4. Protein expression of MDR1 in MDR1-expressing hiPS-BMECs and mock hiPS-BMECs. (A) Comparison of transporter expression levels in MDR1-expressing hiPS-BMECs and mock hiPS-BMECs by SWATH-MS analysis. The solid line passing through the origin represents equal expression levels. Each value represents the mean ± SE from three independent experiments (n = 3). (B) Confocal microscopy of MDR1 in MDR1-expressing hiPS-BMECs and mock hiPS-BMECs. Red and blue signals represent MDR1 and nuclei, respectively. (a) and (b) in panel B indicate the apical and basolateral sides, respectively.

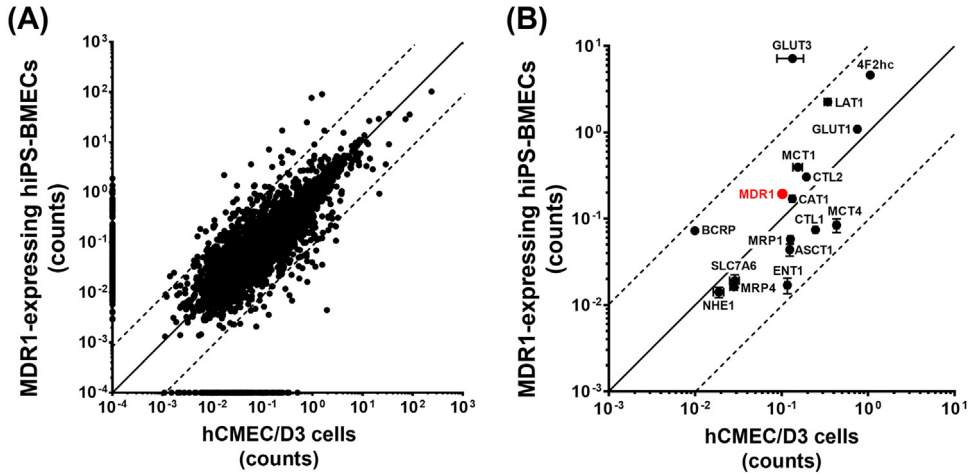

Figure 5. Comparison of comprehensive and transporter protein expression in MDR1-expressing hiPS-BMECs and hCMEC/D3 cells. (A) Comprehensive protein expression by SWATH-MS analysis in MDR1-expressing hiPS-BMECs and hCMEC/D3 cells. (B) Transporter expression among detected all proteins in MDR1-expressing hiPS-BMECs and hCMEC/D3 cells. The solid line passing through the origin represents equal expression levels, and the dot lines represent 10-fold differences. Each value represents the mean ± SE from three independent experiments (n = 3); BCRP in hCMEC/D3 cells (n = 2).

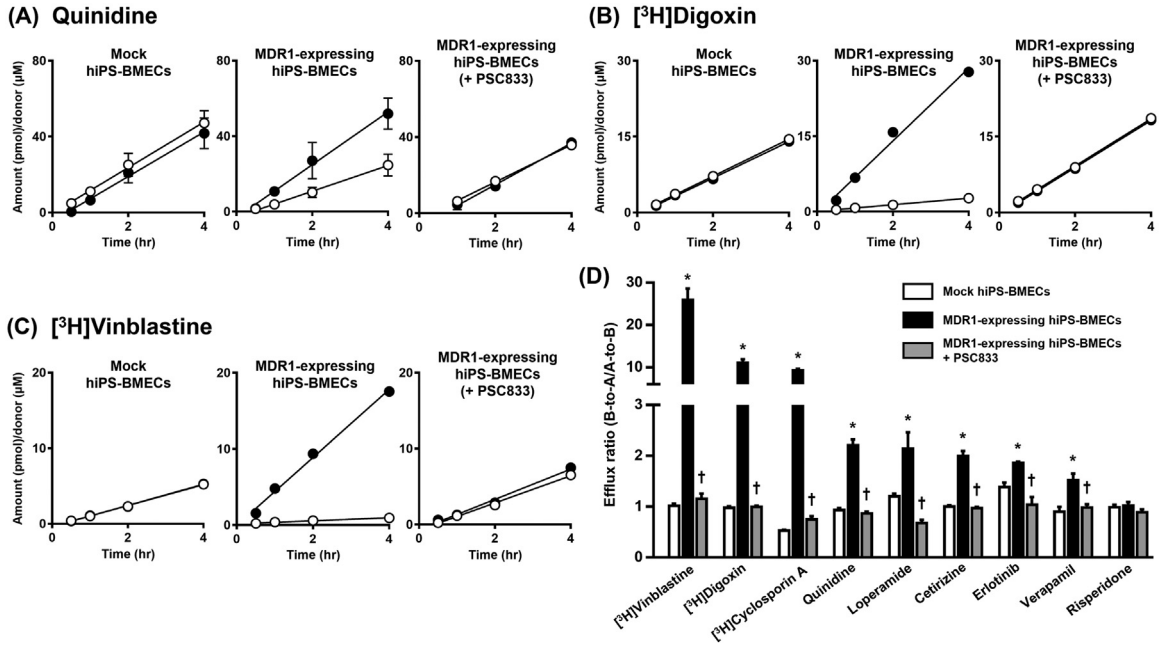

Figure 6. Transport study of MDR1 substrates in MDR1-expressing hiPS-BMECs. Time courses of transport of MDR1 substrates, quinidine (A), [^{3}H]digoxin (B), and [^{3}H]vinblastine (C), across mock hiPS-BMECs and MDR1-expressing hiPS-BMECs monolayers. Transport amount was calculated by dividing drug amount (pmol) by donor drug concentration (μM), and was plotted on the graph. Open and closed circles show transport amounts in the A-to-B and B-to-A directions, respectively. (D) The efflux ratio of MDR1 substrate was calculated in mock hiPS-BMECs and MDR1-expressing hiPS-BMECs with or without MDR1-specific inhibitor. Each value represents the mean ± SE from three to six independent experiments (n = 3-6). Statistical analysis was carried out using the unpaired Student's *t*-test (*$p < 0.05$; mock hiPS-BMECs vs MDR1-expressing hiPS-BMECs, †$p < 0.05$; MDR1-expressing hiPS-BMECs vs 10 μM PSC833).

L-glutamate (0.503, 0.511) (Table 1). In addition, Table 1 shows that dantrolene transport in the B-to-A direction was greater than that in the A-to-B direction, and the P_{app} values were comparable in mock hiPS-BMECs and MDR1-expressing hiPS-BMECs, with ER values of 5.10 and 4.76, respectively.

Discussion

Human-derived *in vitro* models that closely mimic the functional properties of the BBB would be helpful for predicting drug distribution to the human CNS as a part of the drug development process. I n this study, we prepared MDR1-expressing hiPS-BMECs as candidate human BBB models, and evaluated the mRNA and protein expression levels and functional activities of MDR1. We also examined the function and expression of several ABC and SLC transporters expressed at the BBB.

We previously demonstrated that in adenovirus vector systems, the gene expression efficiency of the human polypeptide chain elongation factor-1 alpha (EF-1α) promoter is greater than that of the cytomegalovirus (CMV) promoter in human pluripotent stem cells.[29] Furthermore, in lentivirus vector systems, the EF-1α promoter robustly drives transgene expression in human embryonic stem cells,[30,31] indicating that it shows strong transduction ability in human pluripotent stem cells. Indeed, we found that the number of

Table 1
P_{app} for substrates of SLC transporters or BCRP.

Substrate	Condition	P_{app} ($\times 10^{-6}$ cm/s)		Efflux ratio (B-to-A/A-to-B)
		A-to-B	B-to-A	
[^{3}H]L-Arginine	Mock hiPS-BMECs	6.10 ± 0.82	4.60 ± 0.34	0.754
(3 μCi/mL)	MDR1-expressing hiPS-BMECs	5.86 ± 0.73	4.58 ± 0.46	0.780
[^{14}C]L-Lactate	Mock hiPS-BMECs	36.0 ± 2.9	2.88 ± 0.12	0.0799
(1 μCi/mL)	MDR1-expressing hiPS-BMECs	33.1 ± 2.1	2.36 ± 0.20	0.0711
[^{3}H]L-Leucine	Mock hiPS-BMECs	5.14 ± 0.82	4.66 ± 0.39	0.907
(3 μCi/mL)	MDR1-expressing hiPS-BMECs	6.40 ± 0.78	5.30 ± 0.42	0.829
[^{3}H]L-Glutamate	Mock hiPS-BMECs	5.37 ± 0.18	2.71 ± 0.05	0.503
(3 μCi/mL)	MDR1-expressing hiPS-BMECs	6.02 ± 0.22	3.07 ± 0.05	0.511
Dantrolene	Mock hiPS-BMECs	2.92 ± 0.01	14.9 ± 0.45	5.10
(2 μM)	MDR1-expressing hiPS-BMECs	2.62 ± 0.12	12.5 ± 0.62	4.76

The P_{app} values of several substrates across monolayers of mock hiPS-BEMCs and MDR1-expressing hiPS-BMECs were estimated. Each value is the mean ± SE from three independent experiments (n = 3). P_{app} for [^{14}C]L-lactate was determined with the apical side at pH 6.0 and the basolateral side at pH 7.4. The efflux ratio was calculated as the ratio of $P_{app,\ B\text{-}to\text{-}A}$ and $P_{app,\ A\text{-}to\text{-}B}$. A, apical side; B, basolateral side.

Venus-positive cells obtained by lentiviral transduction was significantly lower in MDR1-overexpressing hiPSCs using CMV promoter than in those using EF-1α promoter (data not shown). Therefore, in this study, we used EF-1α promoter to generate MDR1-overexpressing hiPSCs. We also confirmed the functionality of MDR1 in MDR1-expressing hiPS-BMECs.

Our studies established that MDR1-overexpressing hiPSCs were undifferentiated (Fig. 2), and that MDR1 overexpression in hiPSCs had no significant effect on the physiological barrier function and ABC and SLC transporters expression of mock hiPS-BMECs (Fig. 3 and Fig. 4A), indicating that the functionality of hiPSCs and hiPS-BMECs was unaffected by MDR1 overexpression.

In order to evaluate protein expression of the transporter in MDR1-expressing hiPS-BMECs and mock hiPS-BMECs, SWATH-MS analysis was performed (Fig. 4A). Only MDR1 expression was markedly increased in MDR1-expressing hiPS-BMECs, suggesting that gene transduction to hiPSCs using the present method has no marked effect on the expression of transporter proteins other than MDR1. This is consistent with our finding that neither the ability to form tight junctions nor the cell morphology was changed in MDR1-expressing hiPS-BMECs compared with mock hiPS-BMECs (Fig. 3). Interestingly, in z-axis analysis of the immunocytochemical data, MDR1 signals were detected near the apical membrane rather than in the nucleus, indicating that it is expressed predominantly at the blood-side plasma membrane (Fig. 4B). This is consistent with the localization in human and rodent BBB[32,33] and indicates that the expressed MDR1 should work efficiently to prevent entry of xenobiotics/drugs into the cells from the blood side in MDR1-expressing hiPS-BMECs on culture inserts.

One of the most important issues in the present study is to ascertain whether the newly generated MDR1-expressing hiPS-BMECs could be a useful model cell line for evaluating the function of the human BBB and for preclinical testing in drug development. In order to answer this question, the protein expression levels of MDR1-expressing hiPS-BMECs were comprehensively quantified using the SWATH-MS method and compared with those of hCMEC/D3 cells. The hCMEC/D3 cell line is a widely used BBB model.[9,10] Of the 6077 proteins detected, the expression levels of 90.8% were within a 10-fold difference range between MDR1-expressing hiPS-BMECs and hCMEC/D3 cells (Fig. 5A). In particular, transporters, including MDR1 protein, that determine the transport function in the human BBB were all within the 10-fold difference range in comparison to hCMEC/D3 cells, except for GLUT3 (Fig. 5B). These results suggest that MDR1-expressing hiPS-BMECs should be a good cell model of the human BBB, at least in terms of transporter expression levels. In addition, previous studies reported that the expression levels of transporter proteins in hCMEC/D3 cells correlate with those in isolated human brain capillaries.[8,34] Considering that the TEER value of MDR1-expressing hiPS-BMECs is much higher than that of hCMEC/D3 cells, MDR1-expressing hiPS-BMECs should be useful for evaluation of directional transport during drug development.

The directional transport analysis indicated that the B-to-A transport of typical substrates of MDR1, such as quinidine, [^{3}H]digoxin and [^{3}H]vinblastine, is higher than the A-to-B transport in MDR1-expressing hiPS-BMECs, indicating that efflux transport occurs (Fig. 6A-C). The efflux function of MDR1 in MDR1-expressing hiPS-BMECs was also confirmed by the attenuation of efflux-dominant transport in the presence of PSC833, a specific inhibitor of MDR1. The ER values of MDR1 substrates [^{3}H]cyclosporin A, loperamide, cetirizine, erlotinib, and verapamil are also consistent with efflux transport mediated by MDR1 (Fig. 6D). The profile of ER values for MDR1 substrate drugs in this study was similar to those reported for Caco-2 and MDCK cells; in particular, MDR1-expressing hiPS-BMECs showed lower ER values for quinidine and verapamil than for vinblastine and digoxin.[35,36] In addition, in the directional transport analysis, MDR1-expressing hiPS-BMECs exhibited no significant change of ER value for risperidone, and it is conceivable that other transporters are involved in the transport of risperidone.

Directional transport analysis was also performed for dantrolene, [^{3}H]L-arginine, [^{14}C]L-lactate, [^{3}H]L-leucine, and [^{3}H]L-glutamate, which are typical substrates of breast cancer resistance protein (BCRP/ABCG2), cationic amino acid transporter 1 (CAT1/SLC7A1), monocarboxylate transporter 1 (MCT1/SLC16A1), L-type amino acid transporter 1 (LAT1/SLC7A5) and glutamate aspartate transporter (GLAST/SLC1A3), respectively (Table 1). The obtained values of P_{app} and ER in MDR1-expressing hiPS-BMECs were closely similar to those in mock hiPS-BMECs (Table 1), and the MDR1-expressing hiPS-BMECs and mock hiPS-BMECs exhibited similar TEER values of approximately 3000 $\Omega \times cm^2$, corresponding to strong tight junctions, suggesting that expression of MDR1 protein had no marked influence on the function of transporters or the formation of tight junctions in MDR1-expressing hiPS-BMECs.

Conclusions

In the present study, MDR1-expressing hiPS-BMECs were established as an *in vitro* BBB model with good retention of the functions of the human BBB, including MDR1 efflux function, formation of tight junctions and SLC transporter function. This model is expected to be useful for studies of human BBB function in physiological and pathological conditions, as well as contributing to the development of CNS drugs.

Declaration of Competing Interest

The authors declare that they have no known competing financial interests or personal relationships that could have appeared to influence the work reported in this paper.

Acknowledgments

We would like to thank Masashi Sakuramoto (Laboratory for Medicinal Chemistry Research, Shionogi & Co., Ltd., Osaka, Japan) for technical assistance and data acquisition, and also thank Dr. Pierre-Couraud (Instiut Cochin, Paris, France) for supplying hCMEC/D3 cells under license from INSERM.

Funding

This study was supported by a Grant-in-Aid from the Japan Society for the Promotion of Science (JSPS) KAKENHI (Grant Numbers 22H02790 (YD), 21K20736 (TY), and 21K15321 (TK)), Incubation Grants of Advanced Comprehensive Research Organization (ACRO) of Teikyo University (KT), the Japan Agency for Medical Research and Development (AMED) under Grant Number 22be1004101 (KK), and AMED BINDS 22ama121018 (SO).

Supplementary Materials

Supplementary material associated with this article can be found in the online version at doi:10.1016/j.xphs.2023.09.004.

References

1. Weiss N, Miller F, Cazaubon S, Couraud PO. The blood-brain barrier in brain homeostasis and neurological diseases. *Biochim Biophys Acta*. 2009;1788:842–857.
2. Al Ahmad A, Taboada CB, Gassmann M, Ogunshola OO. Astrocytes and pericytes differentially modulate blood-brain barrier characteristics during development and hypoxic insult. *J Cereb Blood Flow Metab*. 2011;31:693–705.
3. Al Ahmad A, Gassmann M, Ogunshola OO. Maintaining blood-brain barrier integrity: pericytes perform better than astrocytes during prolonged oxygen deprivation. *J Cell Physiol*. 2009;218:612–622.
4. Helms HC, Abbott NJ, Burek M, et al. In vitro models of the blood-brain barrier: an overview of commonly used brain endothelial cell culture models and guidelines for their use. *J Cereb Blood Flow Metab*. 2016;36:862–890.
5. Naik P, Cucullo L. In vitro blood-brain barrier models: current and perspective technologies. *J Pharm Sci*. 2012;101:1337–1354.
6. Deli MA, Abraham CS, Kataoka Y, Niwa M. Permeability studies on in vitro blood-brain barrier models: physiology, pathology, and pharmacology. *Cell Mol Neurobiol*. 2005;25:59–127.
7. Hoshi Y, Uchida Y, Tachikawa M, Inoue T, Ohtsuki S, Terasaki T. Quantitative atlas of blood-brain barrier transporters, receptors, and tight junction proteins in rats and common marmoset. *J Pharm Sci*. 2013;102:3343–3355.
8. Uchida Y, Ohtsuki S, Katsukura Y, Ikeda C, Suzuki T, Kamiie J, Terasaki T. Quantitative targeted absolute proteomics of human blood-brain barrier transporters and receptors. *J Neurochem*. 2011;117:333–345.
9. Weksler B, Romero IA, Couraud PO. The hCMEC/D3 cell line as a model of the human blood brain barrier. *Fluids Barriers CNS*. 2013;10:16.
10. Weksler BB, Subileau EA, Perriere N, et al. Blood-brain barrier-specific properties of a human adult brain endothelial cell line. *FASEB J*. 2005;19:1872–1874.
11. Biemans EALM, Jäkel L, de Waal RMW, Kuiperij HB, Verbeek MM. Limitations of the hCMEC/D3 cell line as a model for Aβ clearance by the human blood-brain barrier. *J Neurosci Res*. 2017;95:1513–1522.
12. Lippmann ES, Azarin SM, Kay JE, et al. Derivation of blood-brain barrier endothelial cells from human pluripotent stem cells. *Nat Biotechnol*. 2012;30:783–791.
13. Lippmann ES, Al-Ahmad A, Azarin SM, Palecek SP, Shusta EV. A retinoic acid-enhanced, multicellular human blood-brain barrier model derived from stem cell sources. *Sci Rep*. 2014;4:4160–4169.
14. Kurosawa T, Tega Y, Higuchi K, et al. Expression and functional characterization of drug transporters in brain microvascular endothelial cells derived from human induced pluripotent stem cells. *Mol Pharm*. 2018;12:5546–5555.
15. Mochizuki T, Mizuno T, Kurosawa T, et al. Functional investigation of solute carrier family 35, member F2, in three cellular models of the primate blood-brain barrier. *Drug Metab Dispos*. 2021;49:3–11.
16. Kurosawa T, Tega Y, Sako D, et al. Transport characteristics of 6-mercaptopurine in brain microvascular endothelial cells derived from human induced pluripotent stem cells. *J Pharm Sci*. 2021;110:3484–3490.
17. Kurosawa T, Sako D, Tega Y, et al. Construction and functional evaluation of a three-dimensional blood–brain barrier model equipped with human induced pluripotent stem cell-derived brain microvascular endothelial cells. *Pharm Res*. 2022;39:1535–1547.
18. Lin JH. How significant is the role of P-glycoprotein in drug absorption and brain uptake? *Drugs Today*. 2004;40:5–22.
19. Delsing L, Donnes P, Sanchez J, et al. Barrier properties and transcriptome expression in human iPSC-derived models of the blood-brain barrier. *Stem Cells*. 2018;36:1816–1827.
20. Yamaguchi T, Nishijima M, Kawabata K. Inhibition of glycogen synthase kinase 3ss enhances functions of induced pluripotent stem cell-derived brain microvascular endothelial cells in the blood-brain barrier. *Biol Pharm Bull*. 2022;45:1525–1530.
21. Zhang H, Yamaguchi T, Kawabata K. The maturation of iPS cell-derived brain microvascular endothelial cells by inducible-SOX18 expression. *Fluids Barriers CNS*. 2023;20:10.
22. Yu J, Vodyanik MA, Smuga-Otto K, et al. Induced pluripotent stem cell lines derived from human somatic cells. *Science*. 2007;318:1917–1920.
23. Miyoshi H, Takahashi M, Gage FH, Verma IM. Stable and efficient gene transfer into the retina using an HIV-based lentiviral vector. *Proc Natl Acad Sci USA*. 1997;94:10319–10323.
24. Miyoshi H, Blomer U, Takahashi M, Gage FH, Verma IM. Development of a self-inactivating lentivirus vector. *J Virol*. 1998;72:8150–8157.
25. Kokubu Y, Yamaguchi T, Kawabata K. In vitro model of cerebral ischemia by using brain microvascular endothelial cells derived from human induced pluripotent stem cells. *Biochem Biophys Res Commun*. 2017;486:577–583.
26. Masuda T, Tomita M, Ishihama Y. Phase transfer surfactant-aided trypsin digestion for membrane proteome analysis. *J Proteome Res*. 2008;7:731–740.
27. Masuda T, Hoshiyama T, Uemura T, et al. Large-scale quantitative comparison of plasma transmembrane proteins between two human blood-brain barrier model cell lines, hCMEC/D3 and HBMEC/ciβ. *Mol Pharm*. 2019;16:2162–2171.
28. Demichev V, Messner CB, Vernardis SI, Lilley KS, Ralser M. DIA-NN: neural networks and interference correction enable deep proteome coverage in high throughput. *Nat Methods*. 2020;17:41–44.
29. Tashiro K, Kawabata K, Inamura M, et al. Adenovirus vector-mediated efficient transduction into human embryonic and induced pluripotent stem cells. *Cell Reprogram*. 2010;12:501–507.
30. Kim S, Kim GJ, Miyoshi H, et al. Efficiency of the elongation factor-1alpha promoter in mammalian embryonic stem cells using lentiviral gene delivery systems. *Stem Cells Dev*. 2007;16:537–545.
31. Ma Y, Ramezani A, Lewis R, Hawley RG, Thomson JA. High-level sustained transgene expression in human embryonic stem cells using lentiviral vectors. *Stem Cells*. 2003;21:111–117.
32. Virgintino D, Robertson D, Errede M, et al. Expression of P-glycoprotein in human cerebral cortex microvessels. *J Histochem Cytochem*. 2002;50:1671–1676.
33. Soontornmalai A, Vlaming MLH, Fritschy JM. Differential, strain-specific cellular and subcellular distribution of multidrug transporters in murine choroid plexus and blood-brain barrier. *Neuroscience*. 2006;138:159–169.
34. Ohtsuki S, Ikeda C, Uchida Y, et al. Quantitative targeted absolute proteomic analysis of transporters, receptors and junction proteins for validation of human cerebral microvascular endothelial cell line hCMEC/D3 as a human blood–brain barrier model. *Mol Pharm*. 2013;10:289–296.
35. Hellinger E, Veszelka S, Tóth AE, et al. Comparison of brain capillary endothelial cell-based and epithelial (MDCK-MDR1, Caco-2, and VB-Caco-2) cell-based surrogate blood-brain barrier penetration models. *Eur J Pharm Biopharm*. 2012;82:340–351.
36. Troutman MD, Thakker DR. Novel experimental parameters to quantify the modulation of absorptive and secretory transport of compounds by P-glycoprotein in cell culture models of intestinal epithelium. *Pharm Res*. 2003;20:1210–1224.